Research in Marine Sciences
Volume 10-Issue 1-2025
Pages 667-684

Impact of Diel Vertical Migration (DVM) on Sardinella aurita retention in the northern Gulf of Guinea

Hilaire Amemou[1, *], Kouacou Bosson[2], and Mamadou Koné[2, 3]

[1]UFR of Marine Sciences, University of San Pedro, San Pedro, Côte d'Ivoire

[2]Laboratory of Matter Sciences, Environment and Solar Energy (LASMES), University Felix Houphouet-Boigny of Cocody-Abidjan, 22 BP 582 Abidjan 22, Abidjan, Côte d'Ivoire

[3]Laboratory of Environmental Sciences and Techniques (LSTE), University Jean-Lorougnon Guédé, Daloa, Côte d'Ivoire

Received: 2024-12-28 *Accepted: 2025-02-19*

Abstract

In the northern Gulf of Guinea, little is known about the Diel Vertical Migration (DVM) of *Sardinella aurita* (*S. aurita*) and its role in reaching suitable nursery sites from spawning locations, as well as the connectivity between these nursery sites and spawning areas. In this study, a biophysical larval dispersal model (Ichthyop), forced by the CROCO (Coastal and Regional Ocean COmmunity) hydrodynamic model was applied, to investigate the impact of DVM on the recruitment of *S. aurita* larvae. Several types of simulation experiments were conducted. These types of simulation experiments were chosen based on previous studies. The first simulation is based on Lagrangian (passive) transport without DVM, while the others include DVM. The results of the simulations revealed that the areas and periods most favorable for recruitment correspond to those identified in previous studies conducted in the region. Additionally, the application of DVM leads to a significant reduction in the number of recruited larvae compared to the simulation without DVM. The simulations indicate that the DVM at different depths (0-25 m, 0-50 m, and 0-75 m) shows similar results, suggesting that S. *aurita* larvae generally remain close to the surface. This is consistent with data showing that *S. aurita*

* Corresponding Author's Email : yagoamemou@gmail.com

spawns mostly in the upper 50 meters of the water column in the northern Gulf of Guinea. The Lagrangian analysis also reveals connectivity between the Cape Palmas and Cape Three Points regions, which is crucial for the conservation of *S. aurita* stocks in the northern Gulf of Guinea.

Keywords: Hydrodynamic model; Larval model; Diel Vertical Migration; S. aurita; Recruitment; Connectivity.

1. Introduction

Sardinella aurita (*S. aurita*) is the dominant small pelagic species in the Ivorian-Ghanaian upwelling ecosystems, and represents a crucial fishery for West African nations (Sarr *et al*., 2019). The variability in recruitment for this species is primarily influenced by environmental conditions, as well as spawning and larval behavior (Mbaye *et al*., 2015; Koné *et al*., 2017). Traditional stock-based approaches are inadequate for modeling the dynamics of small pelagic fish due to their short lifespan and the substantial fluctuations in their abundance. Integrating a hydrodynamic model with an Individual-Based Model (IBM) is essential, as it accounts for environmental heterogeneity and individual variations.

Numerous studies have employed these modeling approaches to analyze the dispersal and recruitment success of small pelagic fish larvae (Dias *et al*., 2014; Mbaye *et al*., 2015; Santos *et al*., 2018). However, in the northern region of the Gulf of Guinea, very few studies have used this approach. Recently, Koné *et al*. (2017) applied a larval dispersion model to study the growth of *S. aurita* larvae along the northern coast of the Gulf of Guinea, but they did not account for the Diel Vertical Migration (DVM) of the larvae.

In this study, the DVM is incorporated to gain a more comprehensive understanding of *S. aurita* larval dynamics, whose reproductive strategy is well adapted to the environmental conditions of the Ivorian-Ghanaian ecosystem. The research is specifically focused on how the DVM of *S. aurita* larvae influences their survival and the efficiency of their transport from spawning areas to recruitment sites. The results of the simulations are then discussed in the context of *S. aurita* reproduction in the northern Gulf of Guinea.

2. Materials and methods

2.1. Hydrodynamic model

The outputs of the Coastal and Regional Ocean COmmunity model (CROCO) are used as the hydrodynamic model. CROCO is an oceanic model built on ROMS_AGRIF and the non-hydrostatic kernel of SNH (Debreu *et al*., 2012), aimed at simulating high-resolution coastal and regional ocean processes, such as coastal upwelling. It employs a generalized sigma coordinate for the vertical grid (Djakouré *et al*., 2014; Koné *et al*., 2017; Amemou *et al*., 2020).

Outputs from the hydrodynamic model were stored every three days for the northern Gulf of Guinea. More detailed explanation of the implementation of the CROCO model is available in a study by Amemou *et al*., (2020). These outputs were then used as forcing factors for the biophysical larval dispersal model in an offline coupling approach.

2.2. The Ichthyop tool

The dispersal of *S. aurita* larvae using Ichthyop (Lett *et al*., 2008) was studied. A Lagrangian model designed to evaluate the impact of both physical and biological factors on ichthyoplankton dynamics. Ichthyop has been extensively used in the Benguela, Humboldt, and Canary upwelling systems to investigate the recruitment success of larvae from small pelagic fish species (Brochier *et al*., 2011; Koné *et al*., 2013). Although Ichthyop has also been employed to study the coastal retention of *S. aurita* eggs and larvae in the northern Gulf of Guinea (Koné *et al*., 2017), it did not account for DVM as a factor influencing larval survival.

2.3. Simulations of larval dispersal

A series of experiments were conducted in which 5,000 virtual eggs were randomly released over six spawning areas (Figure 1), based on field observations of S. *aurita* distribution (Binet, 1982 ; Roy *et al*., 1989 ; Koné *et al*., 2017) in the region :

- Cape Palmas inshore (CaPin, between isobaths 0-1200 m),
- Cape Palmas offshore (CaPoff, between isobaths 1200-2000 m),
- Cape Three Points inshore (CaTPin, between isobaths 0-1200 m),
- Cape Three Points offshore (CaTPoff, between isobaths 1200-2000 m),
- Mid-East Gulf of Guinea inshore (MEGGin, between isobaths 0-1200 m),
- Inshore area of the North-East Gulf of Guinea (NEGGin, between isobaths 0-1200 m).

To be considered recruited in the larval model, virtual particles had to be within the recruitment area (Figure 1) and aged between 7 and 28 days. The 7-day threshold represents the average age at which particles are thought to actively remain in a favorable area (Ditty *et al*., 1994). The 28-day duration represents the average planktonic larval stage (Mbaye *et al*., 2015; Koné *et al*., 2017).

Three DVM simulations were tested. The first simulation, based on Santos *et al*. (2006), assumes that most actively migrating larvae ascend to the surface layer (0 m) at night, while during the day, the majority are found at approximately 25 m (DVM25). Given the limited depth range of this vertical migration, a second DVM simulation (DVM50) was explored, where larvae migrate from 0 m at night to 50 m during the day (Olivar *et al*., 2001). The final DVM scenario involves migration between 0 m and a deeper depth of 75 m (DVM75). The baseline simulation represents a scenario where there is no DVM, while the second simulation

accounts for DVM in S. aurita larvae. The hot letthal temperature in the study is T= 25°C. The survival rate of each cohort was determined after 28 days of transport (Mbaye *et al*., 2015; Koné *et al*., 2017).

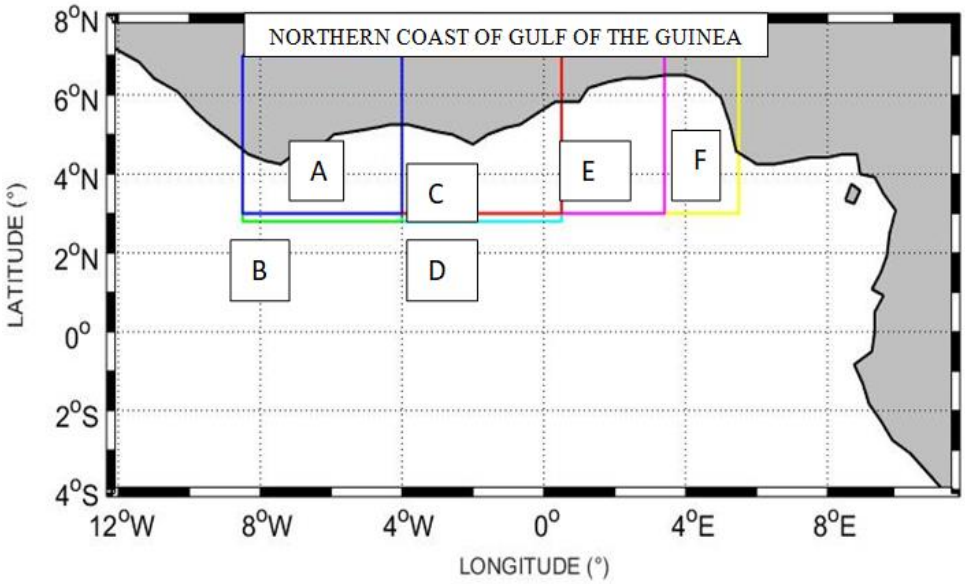

Figure 1. The spawning zones of larvae on the northern coast of the Gulf of Guinea (2°N-6°N). (A) Cape Palmas inshore (CaPin), (B) Cape Palmas offshore (CaPoff), (C) Cape Three Points inshore (CaTPin), (D) Cape Three Points offshore (CaTPoff), (E) Mid-East Gulf of Guinea inshore (MEGGin) and (F) North-East Gulf of Guinea inshore (NEGGin). Recruitment zones are (A) CaPin, (C) CaTPin, (E) MEGGin and (F) NEGGin.

3. Results

The results of two simulations are represented in this section. A simulation that does not account for DVM, and a simulation that incorporates the influence of DVM on the success of larval transport.

3.1. Effect of spawning area of simulated larval retention

The results demonstrate that incorporating a DVM strategy significantly increases larval mortality across all release zones (Figure 2 and Table 1). Recruitment rates show minimal variation between DVM values of 25 m (DVM25), 50 m (DVM50), and 75 m (DVM75) in all regions. In all cases and layers (DVM25, DVM50 and DVM75), the most favorable areas consistently included the inshore regions of CaTPin, MEGGin, and CaPin. The lowest reruitment value was observed for MEGGin across all DVM simulations, while CaPoff exhibited the lowest retention in the simulation without DVM.

3.2. Temporal patterns of simulated larval retention

Figure 3 shows the monthly evolution of simulated larvae recruited across different spawning periods for all cases. As before, recruitment rates are higher in the simulation without DVM than in those with DVM. The seasonality of recruitment rates follows a similar pattern in both the simulation without DVM and across the different DVM values (DVM25, DVM50, DVM75). This consistency underscores the significant impact of DVM on recruitment dynamics, highlighting a need for further investigation into the ecological implications of these behavioral patterns.

Table 1. Percentage of simulated recruitment obtained in the larval model for the different spawning areas and the three layers

	Areas					
Simulations	CaPin (%)	CaPoff (%)	CaTPin (%)	CaTPoff (%)	MEGGin (%)	NEGGin (%)
NO DVM (0-25m)	11	7	11.5	5.5	9.5	0.2
DVM25	9	6	8.5	4.5	8.5	0
NO DVM (0-50 m)	49	22	57	28	48	21
DVM50	8	5	12	9	11	0.2
NO DVM (0-75m)	69	46	82	60	73	69
DVM75	8	5	12	10	12	0.2

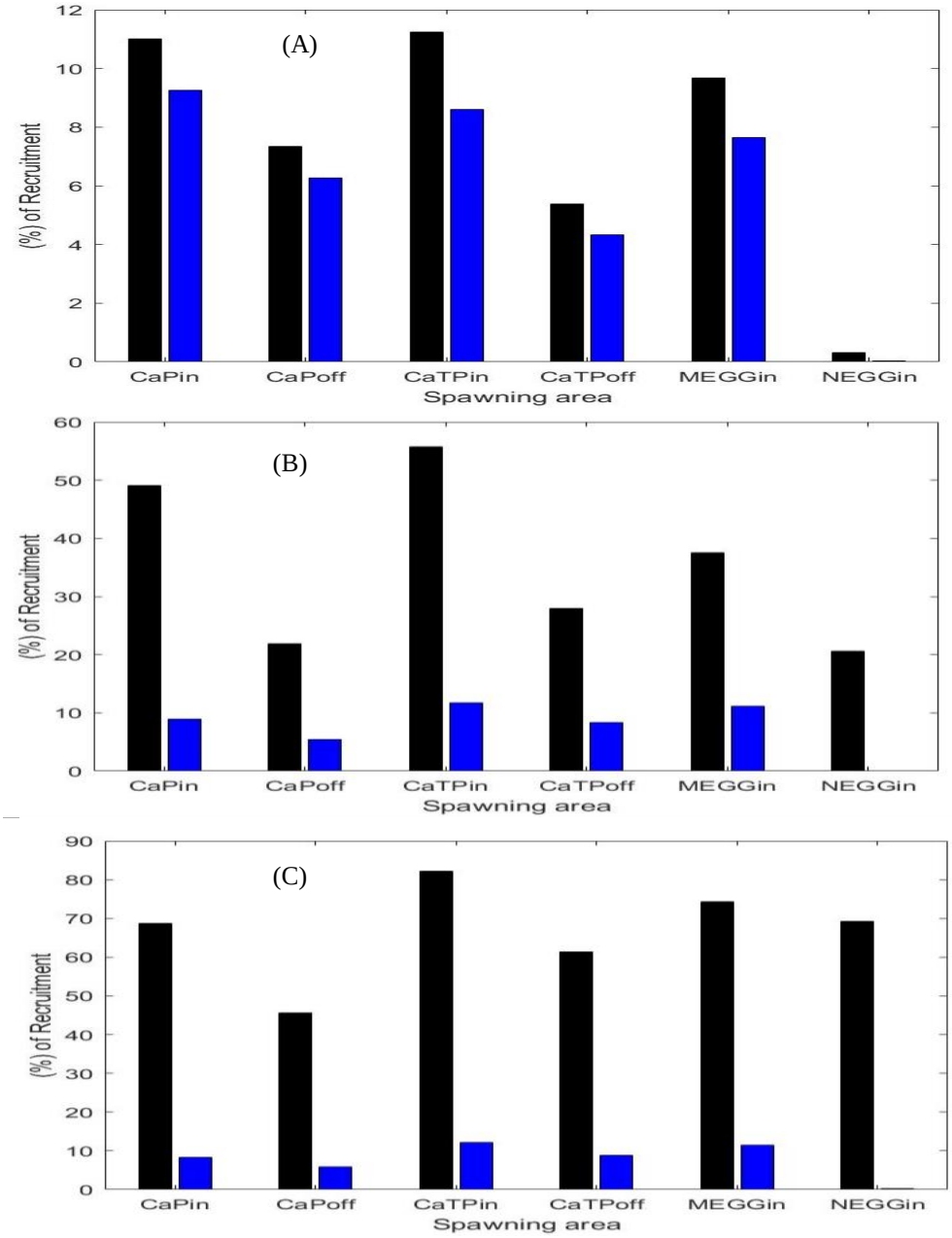

Figure 2. Mean percentage of simulated larvae recruited obtained in the larval model for the different spawning areas and the three layers: (A) 0-25 m, (B) 0-50 m, and (C) 0-75 m. The black bars represent simulations without DVM, while the blue bars correspond to simulations with DVM.

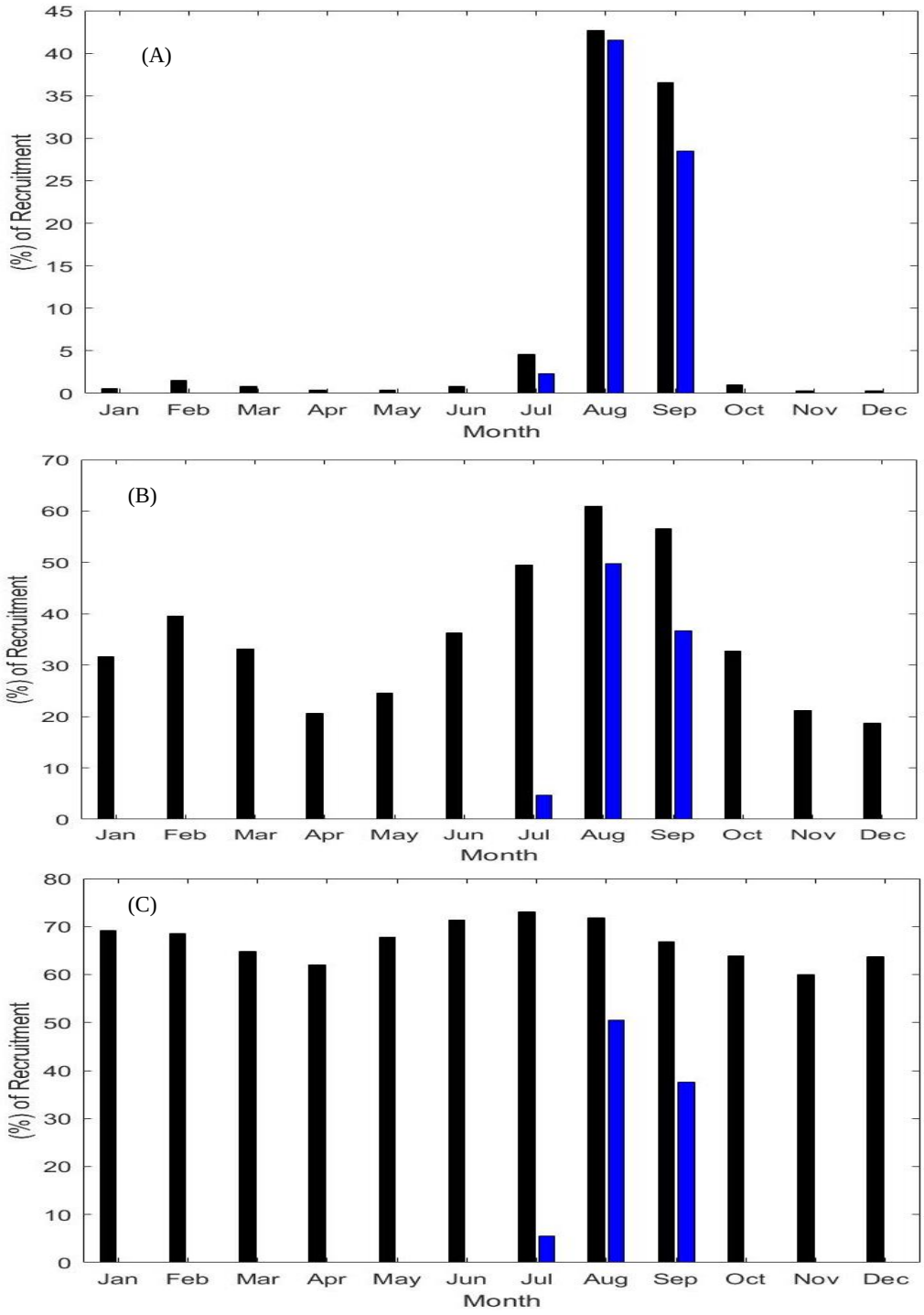

Figure 3. Mean percentage of simulated larvae recruited obtained in the larval model for the different spawning months and the three layers: (A) 0-25 m, (B) 0-50 m, and (C) 0-75 m. The black bars represent simulations without DVM, while the blue bars correspond to simulations with DVM.

The first peak occurs during the minor upwelling period (January to March) in the simulation without DVM. A second, more pronounced peak is observed during the major upwelling period (July to September) across all cases. The surface layer (Figure 3A) exhibits the lowest retention (45%), followed by the intermediate layer (Figure 3B) with a retention rate of 60%, while the deepest layer (Figure 3C) shows the highest retention (80%).

3.3. Effect of spawning depth of simulated larval retention

As with the previous simulations without DVM, the recruitment is higher when eggs are released from deeper depth (Figure 4 and Table 2). In the simulation without DVM, the deepest level (0-75 m, Figure 4C) was the most favorable, with 67%, followed by the intermediate zone (0-50 m, Figure 4B) at 35.5%, and finally, the surface layer (0-25 m, Figure 4A) at 7.5% (Table 2). Recruitment rates show little variation across DVM values of 25 m (DVM25), 50 m (DVM50) and 75 m (DVM75) (around 7 %).

Table 2. Percentage of simulated recruitment obtained from the larval model for the three layers.

Release Depth	0 – 25 m		0 - 50 m		0 - 75 m	
Simulations	NO DVM	DVM25	NO DVM	DVM50	NO DVM	DVM75
Percentage	7.5 %	5.8 %	35.5 %	7.6 %	67 %	7.8 %

3.4. Simulated larval transport and connectivity

This concern is based on analyzing connectivity patterns along the northern coast of the Gulf of Guinea, assessing the transport of eggs and larvae from their spawning sites to other favorable coastal areas to the west or east.

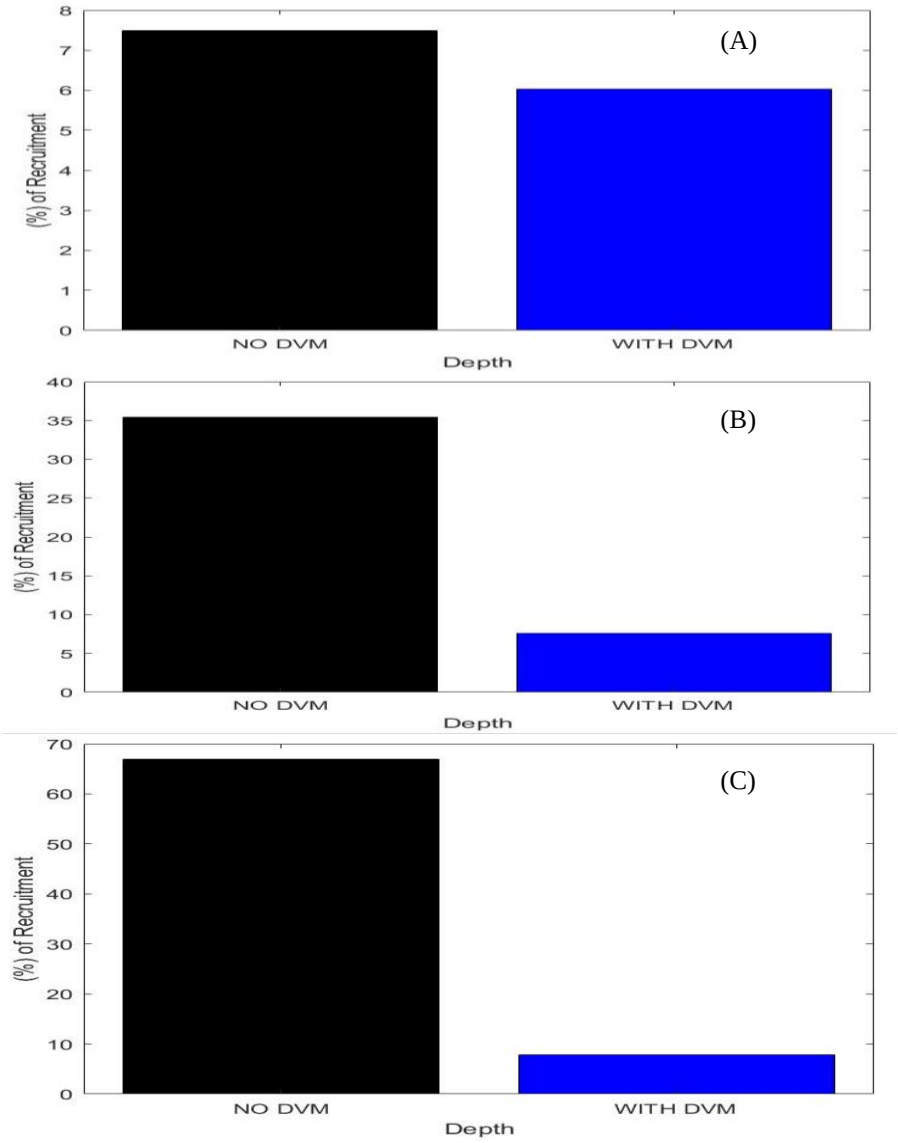

Figure 4. Mean percentage of simulated larvae recruited obtained in the larval model for the different spawning depths and the three layers: (A) 0-25 m, (B) 0-50 m, and (C) 0-75 m. The black bars represent simulations without DVM, while the blue bars correspond to simulations with DVM.

3.4.1 Larval transport along the eastern coast

The exchange of larvae between the two spawning areas in the western part of the domain (CaPin and CaTpin) and the favorable coastal areas to the east (MEGGin and NEGGin) was limited across all layers (Figure 5). The surface layer (Figure 5A) has the lowest percentage of recruited larvae (3%). This exchange typically occurs between July and September (during major upwelling) for all simulations. In all cases, simulations show that fewer than 7% of the surviving individuals (those not advected offshore), released from CaPin and CaTpin (the western region), were transported to the eastern area during summer (Figure 5). The surface

layer (Figure 5A) has the lowest percentage of recruited larvae (3%). The deep layer (Figure 5C) has a recruitment percentage of 4.5%, while the intermediate layer (Figure 5B) exhibits the highest percentage at 6.5% (Figure 5B).

3.4.2 Larval transport along the western coast

Similarly, larval transport is low here, as in the previous cases (Figure 6). In all cases, less than 12% of the eggs released in the eastern area (MEGGin and NEGGin) were transported westward, and this transport occurs during the summer (Figure 6). Once again, the surface layer (Figure 6A) has the lowest percentage of recruited larvae (3%). The deep layer (Figure 6C) shows a recruitment percentage of 9.5%, whereas the intermediate layer displays the highest recruitment at 11.5% (Figure 6B).

3.4.3 Larval transport between the two Capes

This section shows the larval transport between the two upwelling zones (CaPin and CaTPin) located in the northern region of the Gulf of Guinea.

1) From CaPin (spawning area) to CaTPin (recruitment area)

The transport of larvae and eggs from the spawning area (CaPin) to the recruitment area (CaTPin) is similar across all cases.

This process typically occurs during the summer (major upwelling period), with a maximum value of recruited larvae (30%) for the surface layer (0-25 m, Figure 7A). Another period of recruitment is also observed during the minor upwelling season in the simulations without DVM, for the intermediate (0-50 m, Figure 7B) and deep (0–75 m, Figure 7C) layers.

2) From CaTPin (spawning area) to CaPin (recruitment area)

In all cases, simulations show that fewer than 15% of the surviving individuals (not advected offshore) released in the CaTPin region were transported to the CaPin region in summer (Figure 8). During the minor upwelling season, an additional retention period is observed in the simulations without DVM, particularly for the intermediate (0–50 m) and deep (0–75 m) layers. In this case, the surface layer (0–25 m) has the lowest recruitment (0.8%).

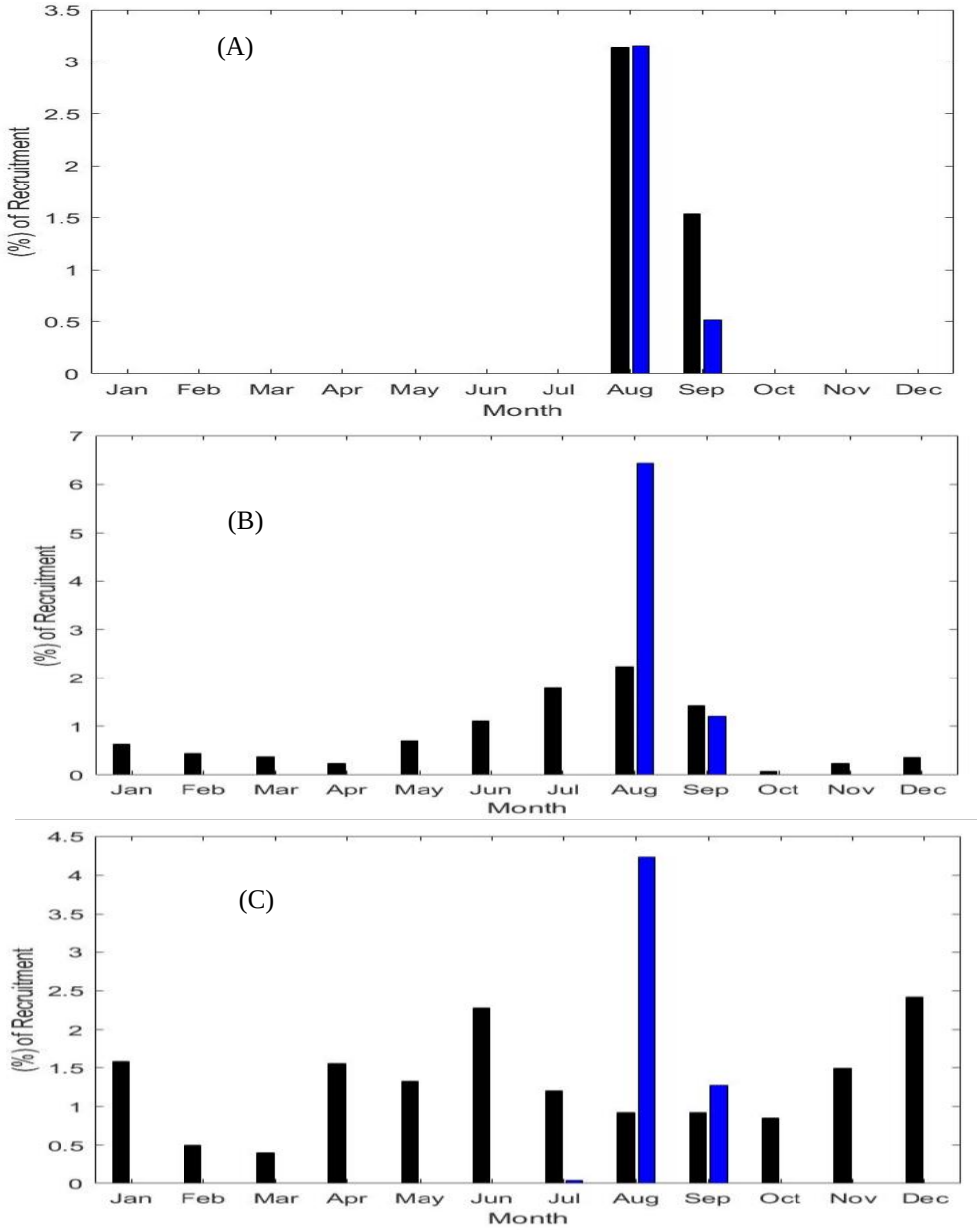

Figure 5. Monthly evolution of the mean percentage of simulated larvae recruited obtained in the larval model for the two spawning areas (CaPin and CaTPin), two favorable areas (MEGGin and NEGGin) and the three layers: (A) 0-25 m, (B) 0-50 m, and (C) 0-75 m. The black bars represent simulations without DVM, while the blue bars correspond to simulations with DVM.

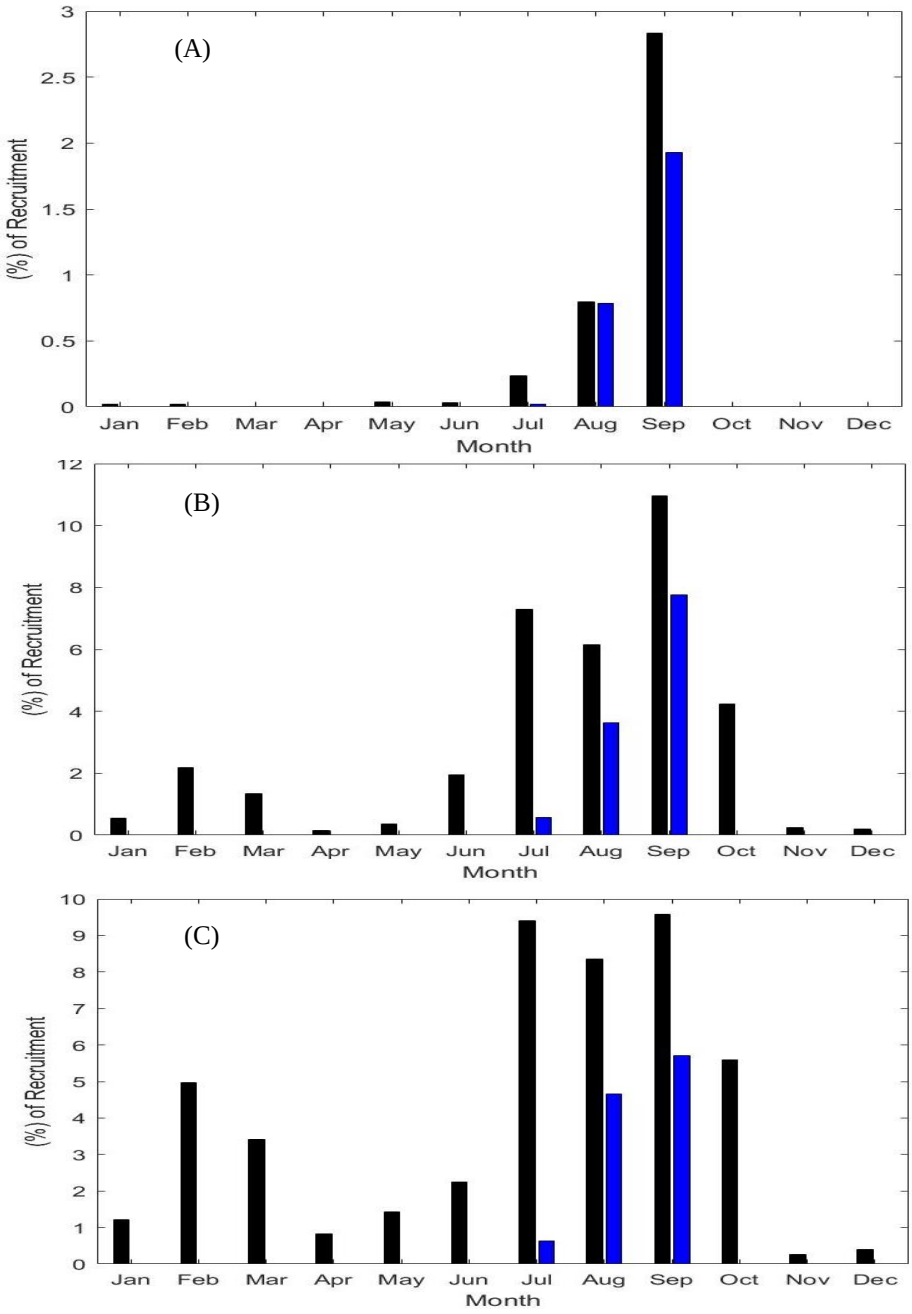

Figure 6. Monthly evolution of the mean percentage of simulated larvae recruited obtained in the larval model for the two spawning areas (MEGGin and NEGGin), two favorable areas (CaPin and CaTPin) and the three layers: (A) 0-25 m, (B) 0-50 m, and (C) 0-75 m. The black bars represent simulations without DVM, while the blue bars correspond to simulations with DVM.

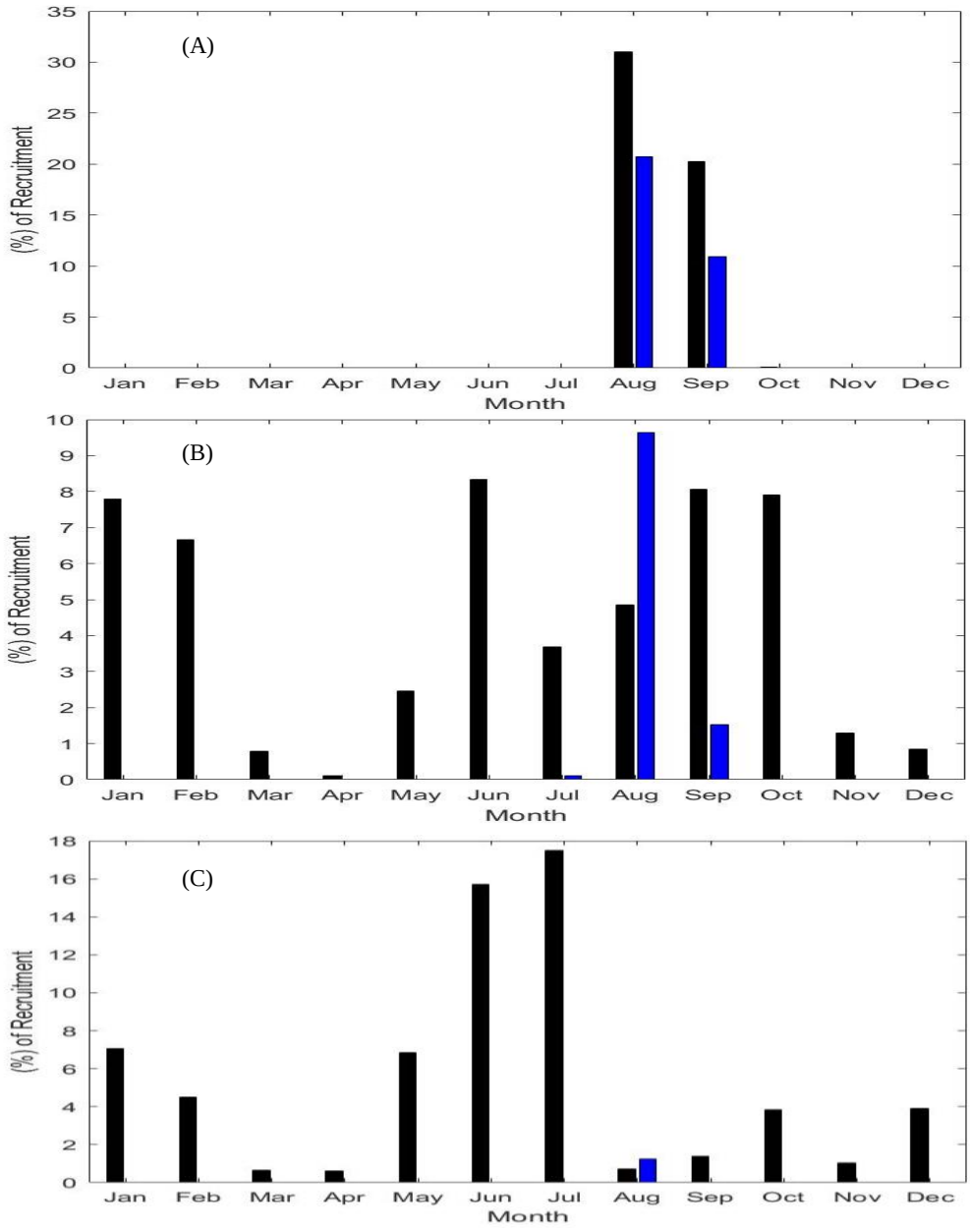

Figure 7. Monthly evolution of the mean percentage of simulated larvae recruited obtained in the larval model for the spawning area (CaPin), the favorable area (CaTPin) and the three layers: (A) 0-25 m, (B) 0-50 m, and (C) 0-75 m. The black bars represent simulations without DVM, while the blue bars correspond to simulations with DVM.

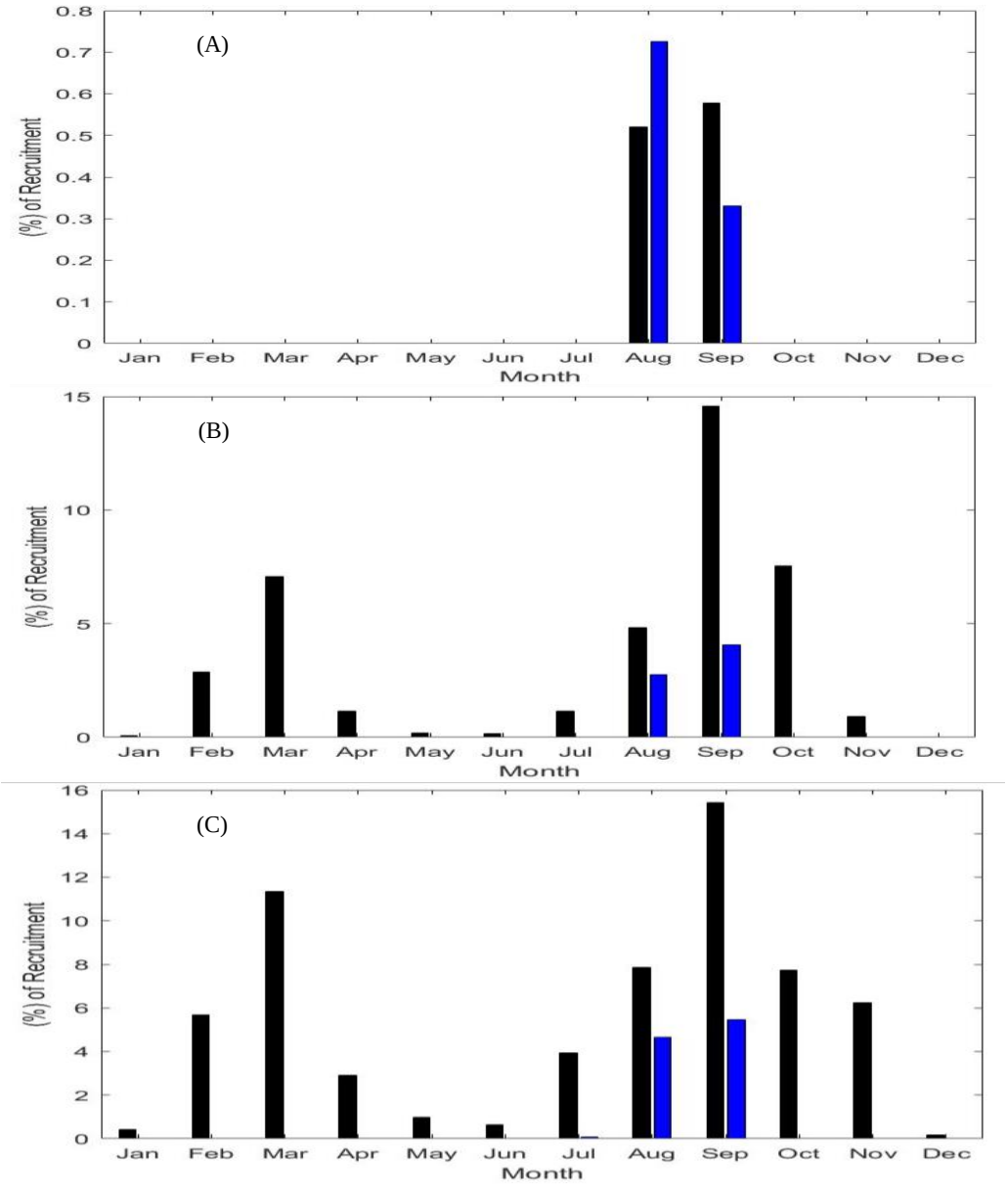

Figure 8. Monthly evolution of the mean percentage of simulated larvae recruited obtained in the larval model for the spawning area (CaTPin), the favorable area (CaPin) and the three layers: (A) 0-25 m, (B) 0-50 m, and (C) 0-75 m. The black bars represent simulations without DVM, while the blue bars correspond to simulations with DVM.

4. Discussions

All DVM simulations have little effect on the spatial retention pattern but slightly increase the offshore transport of larvae. Including DVM significantly decreases the spatial amplitude of simulated larvae recruited in all spawning areas (Figure 2). This can be explained by the fact

that larvae primarily remain in the neuston layer (0 m), where wind effects and offshore transport are more significant (Mbaye *et al*., 2015; Santos *et al*., 2018). The areas most favorable to larval recruitment generally remained the inshore regions (CaTPin, CaPin, and MEGGin), while areas with much lower retention included CaPoff and NEGGin (Figure 2). These findings are consistent with previous studies (Roy *et al*., 1989; Koné *et al*., 2017; Amemou, 2021), which highlight that these regions are particularly conducive to egg and larval recruitment and survival due to eddies that prevent offshore advection and loss. DVM25 shows a lower recruitment rate compared to the other simulations (DVM50 and DVM75) due to the spawning areas being in the 0-25 m depth range, where high offshore advection of eggs and larvae occurs because of the Guinea Current (GC). This current can reach velocities of up to 1 m/s in the surface layers (Richardson and Reverdin, 1987). The velocity of the current decreases with depth, resulting in more favorable conditions for coastal retention in the deeper layers.

In the simulation without DVM, the primary spawning periods observed along the northern coast of the Gulf of Guinea occur during the two upwelling seasons. The first occurs from January to March, with a peak in February during the minor upwelling, while the second, more pronounced peak takes place from July to October during the major upwelling, as highlighted in previous studies (Koné *et al*., 2017; Amemou, 2021). In the simulations with DVM, a peak is observed during the main upwelling season, although its amplitude is lower compared to the simulations without DVM (Figure 3). During the upwelling season, there is an abundance of food and a favorable temperature for larval growth. Consequently, it can be concluded that S. aurita larvae adopt a DVM strategy, driven by both food availability and temperature (Olivar *et al*., 2001; Santos *et al*., 2006). However, the main objective of this study is not to investigate larval survival in relation to food availability, this topic will be explored in future research.

In simulations without DVM (Figure 4), the simulated larvae recruited incease with the depth as in Koné *et al*. (2017). However, the retention does not increase with the depth and the amplitude remains low in the differents layers for DVM simulations (Figure 4). This implies that the larvae are not being held more effectively at greater depths and larvae's movements are confined and not highly variable across different depths. The similarity of the results for DVM at different depths (25 m, 50 m, and 75 m) indicates that the larvae do not typically migrate deeper than 75 meters. This reinforces the idea that the larvae stay within a relatively shallow range of the water column, and are not found at deeper depths. The results align with the findings of Boély and Fréon, (1979), who demonstrated that S. aurita primarily spawns in the upper 50 meters along the northern coast of the Gulf of Guinea. In the Senegal-Mauritanian upwelling system, the study by Mbaye *et al*. (2015) suggests that S. aurita spawns at depths of up to 50 meters.

In all cases, the exchange of larvae between the western regions (CaPin and CaTPin) and the eastern regions (MEGGin and NEGGin) is limited. This indicates that larvae are not being

transported extensively between these areas (Figure 5 and Figure 6). The fact that the larval exchange is weak and only observed during the major upwelling suggests that the upwelling might not be consistently strong enough to drive significant larval movement across regions. During the major upwelling period, the exchange of larvae between the regions of CaPin and CaTPin is greater from CaPin (western side) to CaTPin (eastern side), which indicates that larvae are being transported eastward, from the western region towards the eastern one (Figure 7 and Figure 8). The larval exchange occurs primarily in the surface layer (0-25 m). This suggests that the transport mechanism driving the eastward movement of larvae is likely related to principal surface current (GC), which are more influential at these shallower depths. The increased exchange of larvae in the surface layer during the major upwelling period can be linked to the intensification of the Guinea Current, which flows from west to east along the northern coast of Gulf of Guinea (Bourlès *et al*., 1999; Lumpkin and Garzoli, 2005; Bosson *et al*., 2023). During the upwelling period, this current strengthens, which could enhance the eastward transport of larvae. The current likely acts as a primary mechanism for moving larvae across the regions, particularly within the surface layer where the current has its most direct effect.

Conclusion

The aim of this study is to assess the impact of DVM on the recruitment of *S. aurita* larvae in the northern Gulf of Guinea. DVM plays a crucial role in larval mortality, with the recruited larvae typically remaining near the surface. The results revealed connectivity between the two upwelling zones, particularly in the west-to-east direction, driven by the Guinea current. Future work will incorporate a bioenergetic model for larval growth, accounting for different vertical migration regimes based on larval size. This will enable a more detailed investigation into the biological effects on reproductive success, further exploring how variations in migration behaviors, influenced by larval size, affect growth and overall reproductive outcomes.

References

Amemou, H. 2021. Modélisation biophysique de la dispersion et de la croissance des larves de sardinelles dans le Golfe de Guinée. Sorbonne Université and Université Félix Houphouët-Boigny.

Amemou, H., Koné, V., Aman, A., and Lett, C. 2020. Assessment of a Lagrangian model using trajectories of oceanographic drifters and fishing devices in the Tropical Atlantic Ocean. Progress in Oceanography, 188: 102426. https://doi.org/10.1016/j.pocean.2020.102426.

Binet, D. 1982. Influence des variations climatiques sur la pêcherie des Sardinella aurita ivoiro-ghanéennes: relation sécheresse-surpêche. Oceanologica Acta, 5(4): 443-452.

Boély, T., and Fréon, P. 1979. Les ressources pélagiques côtières. In: Les ressources halieutiques de l'Atlantique centre-est. I. Les ressources du Golfe de Guinée de l'Angola à la Mauritanie., FAO Document Technique Pêches.ed.

Bosson, K., Aman, A., Toualy, E., and Arnault, S. 2023. The surface Guinea Current variability from satellite data. Regional Studies in Marine Science, 64: 103045. https://doi.org/10.1016/j.rsma.2023.103045.

Bourlès, B., Gouriou, Y., and Chuchla, R. 1999. On the circulation in the upper layer of the western equatorial Atlantic. Journal of Geophysical Research, 104: 21151–21170. https://doi.org/10.1029/1999JC900058.

Brochier, T., Mason, E., Moyano, M., Berraho, A., Colas, F., and *et al*. 2011. Ichthyoplankton transport from the African coast to the Canary Islands. Journal of Marine Systems, 87: 109–122. https://doi.org/10.1016/j.jmarsys.2011.02.025.

Debreu, L., Marchesiello, P., Penven, P., and Cambon, G. 2012. Two-way nesting in split-explicit ocean models: Algorithms, implementation and validation. Ocean Modelling, 49–50: 1–21. https://doi.org/10.1016/j.ocemod.2012.03.003.

Dias, D.F., Pezzi, L.P., Gherardi, D.F.M., and Camargo, R. 2014. Modeling the spawning strategies and larval survival of the Brazilian sardine (Sardinella brasiliensis). Progress in Oceanography, 123: 38–53. https://doi.org/10.1016/j.pocean.2014.03.009.

Ditty, J., Houde, E., D., and Shaw, R., F. 1994. Egg and larval development of spanish sardine, Sardinella aurita (Family Clupeidae), with a synopsis of characters to identify clupeid larvae from the northern Gulf of Mexico. Bulletin of Marine Science, 54: 367–380.

Djakouré, S., Penven, P., Bourlès, B., Veitch, J., and Koné, V. 2014. Coastally trapped eddies in the north of the Gulf of Guinea. Journal of Geophysical Research: Oceans, 119: 6805–6819. https://doi.org/10.1002/2014JC010243.

Koné, V., Lett, C., and Fréon, P. 2013. Modelling the effect of food availability on recruitment success of Cape anchovy ichthyoplankton in the southern Benguela upwelling system. African Journal of Marine Science, 35: 151–161. https://doi.org/10.2989/1814232X.2013.796893.

Koné, V., Lett, C., Penven, P., Bourlès, B., and Djakouré, S. 2017. A biophysical model of S. aurita early life history in the northern Gulf of Guinea. Progress in Oceanography, 151: 83–96. https://doi.org/10.1016/j.pocean.2016.10.008.

Lett, C., Verley, P., Mullon, C., Parada, C., Brochier, T., and *et al*. 2008. A Lagrangian tool for modelling ichthyoplankton dynamics. Environmental Modelling & Software, 23: 1210–1214. https://doi.org/10.1016/j.envsoft.2008.02.005.

Lumpkin, R., and Garzoli, S.L. 2005. Near-surface circulation in the Tropical Atlantic Ocean. Deep Sea Research Part I: Oceanographic Research Papers, 52: 495–518. https://doi.org/10.1016/j.dsr.2004.09.001.

Mbaye, B.C., Brochier, T., Echevin, V., Lazar, A., Lévy, M., and *et al*. 2015. Do Sardinella aurita spawning seasons match local retention patterns in the Senegalese–Mauritanian upwelling region? Fisheries Oceanography, 24: 69–89. https://doi.org/10.1111/ fog.12094.

Olivar, M., Salat, J., and Palomera, I. 2001. Comparative study of spatial distribution patterns of the early stages of anchovy and pilchard in the NW Mediterranean Sea. Marine Ecology Progress Series. 217: 111–120. https://doi.org/10.3354/meps217111.

Richardson, P.L., and Reverdin, G. 1987. Seasonal cycle of velocity in the Atlantic North Equatorial Countercurrent as measured by surface drifters, current meters, and ship drifts. Journal of Geophysical Research. 92, 3691. https://doi.org/10.1029/JC092iC04p03691.

Roy, C., Cury, P., Fontana, A., and Belvèze, H. 1989. Stratégies spatio-temporelles de la reproduction des clupéidés des zones d'upwelling d'Afrique de l'Ouest. Aquatic Living Resources. 2: 21–29. https://doi.org/10.1051/alr:1989003.

Santos, A.M.P., Nieblas, A.-E., Verley, P., Teles-Machado, A., Bonhommeau, S., and *et al*. 2018. Sardine (Sardina pilchardus) larval dispersal in the Iberian upwelling system, using coupled biophysical techniques. Progress in Oceanography, 162: 83–97. https://doi.org/10.1016/j.pocean.2018.02.011

Santos, A.M.P., Ré, P., Dos Santos, A., and Peliz, Á. 2006. Vertical distribution of the European sardine (Sardina pilchardus) larvae and its implications for their survival. Journal of Plankton Research, 28: 523–532. https://doi.org/10.1093/plankt/fbi137.

Sarr, A., Ndiaye, W., Faye, A., and Diouf, M. 2019. Age, growth and mortality rates of round sardinella, Sardinella aurita (Valenciennes, 1810) from the Senegalese coasts (West Africa). International Journal of Fisheries and Aquaculture, 11(2): 37-42.